Fault Displacement Simulation Analysis of the Kamishiro Fault Earthquake in Nagano Prefecture Using the Parallel Finite Element Method

Yuta Mitsuhashi[1(✉)], Gaku Hashimoto[2], Hiroshi Okuda[2], and Fujio Uchiyama[1]

[1] Disaster Reduction and Environmental Engineering Deptartment,
Kozo Keikaku Engineering, Inc., 4-5-3 Chuo, Nakano-Ku, Tokyo 164-0011, Japan
`yuta-mitsuhashi@kke.co.jp`
[2] Graduate School of Frontier Sciences, University of Tokyo, 5-1-5 Kashiwanoha,
Kashiwa-shi, Chiba 277-8563, Japan

Abstract. In recent years, the evaluation of fault displacement has been required for evaluating the soundness of underground structures during an earthquake. Fault displacement occurs as the result of the rupture of the earthquake source fault, and studies have been conducted using the finite difference method, the finite element method, etc. The present study used the nonlinear finite element method to perform a dynamic rupture simulation analysis of the Kamishiro fault earthquake in Nagano Prefecture on November 22, 2014. A model was prepared using a solid element for the crust and a joint element for the fault surface. The Kamishiro fault earthquake in Nagano was a reverse-fault earthquake whose fault plane included a part of the Kamishiro fault and extended northward from there. The total extent was 9 km, and the surface fault displacement confirmed was approximately 1 m at maximum. Initial stress was applied to the fault to intentionally rupture the hypocenter to perform a propagation analysis of the rupture, and the displacement and response time history obtained in the analysis were compared with observational records. At this time, joint elements according to Goodman et al. that had been expanded were introduced to the finite element method code FrontISTR, which can analyze large-scale models, and the simulation analysis was performed.

Keywords: Fault distance · FEM · Joint element · Dynamic rupture simulation · Parallel computing

1 Introduction

In recent years, the evaluation of fault displacement has been required for evaluating the soundness of underground structures during an earthquake. Fault displacement occurs as the result of the rupture of the earthquake source fault, and studies have been conducted using the finite difference method (i.e. [1]) and the finite element method (i.e. [2]). In particular, many studies centering on the finite difference method have been performed using dynamic rupture simulation analysis, which reproduces the spontaneous rupture process of a fault using a slip-weakening model (i.e. [1]).

The present study used the 3D nonlinear finite element method to perform a simulation analysis of the Kamishiro fault earthquake in Nagano Prefecture on November 22, 2014. The Kamishiro fault earthquake in Nagano (Mj 6.7, *Mw* 6.2) was a reverse-fault earthquake whose fault plane included a part of the Kamishiro fault and extended northward from there, with a length of approximately 20 km and a depth of approximately 10 km. The total extent was 9 km, and the surface fault displacement confirmed was approximately 1 m at maximum [3]. Also, a maximum acceleration of approximately 600 cm/s^2 was observed in the K-NET [4] observation points near the fault. A 40 km $\times$ 40 km $\times$ 20 km model that included the earthquake source fault was prepared using a solid element for the crust and a joint element for the fault. A model was created for the rupture process of the fault according to the nonlinear constitutive law incorporating stress drop, and for the initial conditions, initial stress was applied to the joint element to rupture the fault, and the ground surface response time history caused by propagation of the rupture was compared with the observational records of K-NET. Also, the surface fault displacement observed in studies of the actual site after the earthquake was compared with the displacement obtained in the present analysis. This research was conducted using the finite element method code FrontISTR [5], which can perform parallel computation of large-scale models. This allowed a wide area of the crust to be analyzed using relatively fine mesh.

2 Analytical Conditions of the 3D Finite Element Method

2.1 Creating a Model of the Fault by Joint Elements

In the present study, a model of the fault was created by the joint elements shown in Fig. 1. Those joint elements are finite elements that easily simulate the contact/sliding/exfoliation between two physical bodies. Several joint elements have been proposed, such as those proposed by Goodman et al. [6] and those that have been formulated on the basis of 3D isoparametric elements. The shape of the elements according to Goodman et al. was hypothesized to be rectangular, and the deformation between the two contacting surfaces is represented by the 6-mode combination shown in Fig. 2. The authors expanded this to the desired shape of a triangle or quadrilateral, and implemented FrontISTR. This allowed a high-precision analysis to be performed, even with distorted mesh.
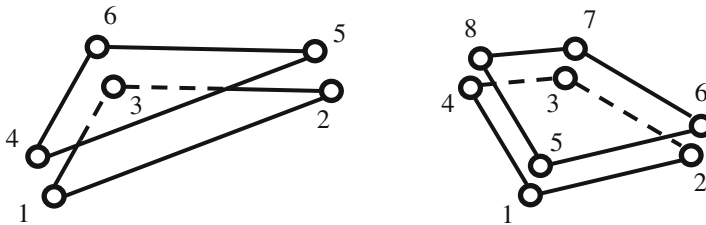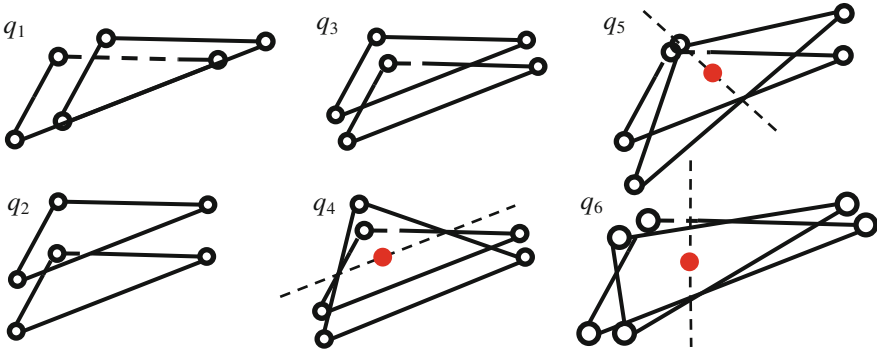

Fig. 1. Joint elements

Fig. 2. Deformation mode of the joint elements

The relationship between the shearing stress and relative displacement of the joint element used in this study is shown in Fig. 3(a). The joint elements have a bi-directional degree of freedom with respect to the translation deformation in the surface (q_1 and q_2 shown in Fig. 2), so the shearing stress τ and the relative displacement ε are evaluated in Eqs. (1) and (2). However, f_{q1} and f_{q2} are the shearing stress according to modes q_1 and q_2, and δ_{q1} and δ_{q2} are the displacement of modes q_1 and q_2.

$$\tau = \sqrt{f_{q_1}^2 + f_{q_2}^2} \tag{1}$$

$$\delta = \sqrt{\delta_{q_1}^2 + \delta_{q_2}^2} \tag{2}$$

As shown in Fig. 3(a), sliding rupture occurs when the shearing stress τ of joint elements reaches the yield stress τ_y, and a stress drop to τ_0 occurs. According to past studies (i.e. [1]), the behavior of the shearing stress after sliding rupture is that it does not rapidly drop to τ_0 but has a certain degree of inclination, and with the slip-weakening model in the finite difference method, a frequently used model is one in which the shearing stress drops linearly to critical slip displacement D_c shown in Fig. 3(b). For convenience sake,
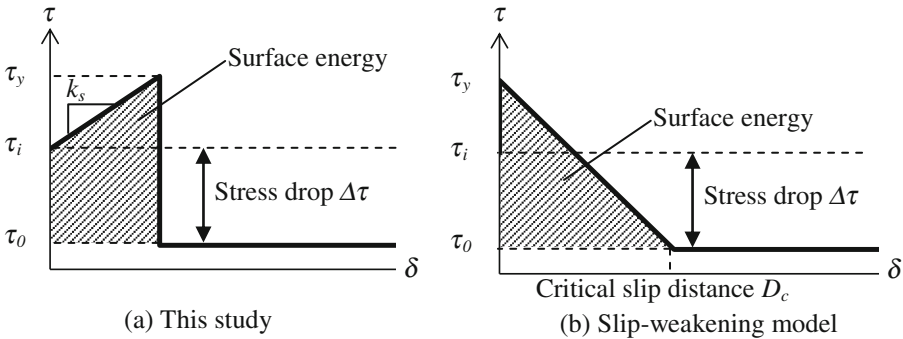

(a) This study   (b) Slip-weakening model

Fig. 3. Stress displacement relationship

the present study used a model in which the shearing stress dropped to τ_0 the instant that sliding rupture occurred. Also, according to past studies [2], the analytical results depend on the relative quantity $\Delta\tau = \tau_y - \tau_0$, not on the absolute quantity τ_0. Therefore, this study used an analysis that focused on the relative value $\Delta\tau$ when $\tau_0 = 0$MPa. In addition, referring to Dan et al. ([1]), the initial shearing stiffness k_s of the joint elements was specified so that the surface energy calculated from $D_c = 25$ cm in the slip-weakening model was equivalent, and the vertical stiffness k_v was made to be linear and a sufficiently rigid value.

2.2 Movement Equation

The movement equation is given by Eq. (3).

$$M\ddot{x} + C\dot{x} + Kx = F \tag{3}$$

Here, x is the displacement; M, C, and K are the mass, damping, and stiffness matrix, respectively; F is the external force vector. For damping, stiffness-proportional damping was used, and referring to the maximum transmission frequency of the model and the study by Mizumoto et al. [2], it was established that there would be 2 % damping at 1 Hz. Also, the effect of the reflected wave was eliminated by setting the viscous boundary to the model periphery that excluded the crust surface. According to the constitutive law of the joint elements shown in Fig. 3(a), this problem had non-linearity, so a convergent calculation according to the Newton-Raphson method was performed.

3 Analysis Model

The model used in analysis is shown in Fig. 4, and the fault parameters are shown in Table 1. The fault shape was established by referring to the AIST active fault database [7] and aftershock distribution, and a strike angle of 12°, dip angle of 50°, length of 18 km, and depth of 10 km (width of 12.2 km) were established. As for generally used physical values, $\nu = 0.25$ was hypothesized with the share modulus of stiffness μ set to 30 GPa and the unit weight γ was set to 2.5 t/m3. Referring to the records on the hypocenter of this earthquake, the hypocenter was set to a position at a 5-km depth, and the τ_y of the joint elements was set at a large value. The Kamishiro fault earthquake was a reverse-fault earthquake. But the earthquake was also indicated to have been accompanied by a left-lateral slip. So we assume the direction of initial stress λ as 90° (pure reverse-fault), 75°, 60° and 45°, and we compare their results(See Fig. 4). By setting an initial stress, rupture would occur at the same time that the analysis started. Since ground surface displacement was not observed on the north side of the fault, the shape of the fault surface might not have been a simple rectangle, but for convenience sake, this study used a rectangular fault.
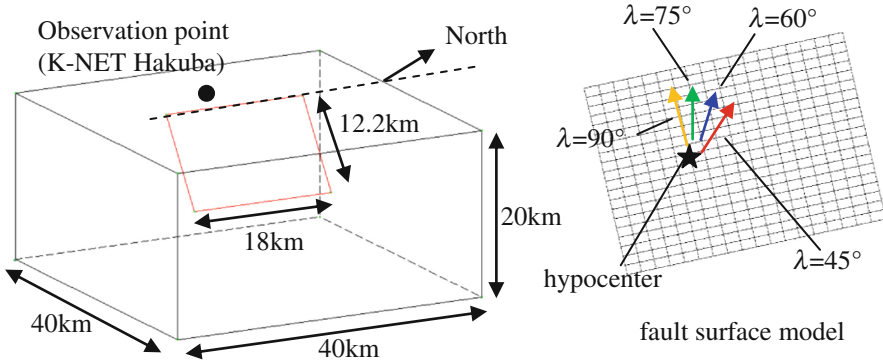
Fig. 4. Analysis model.

Table 1. Fault parameters

Fault width	W	12.2	km
Fault length	L	18.0	km
Strike angle	θ	12	degree
Dip angle	δ	50	degree
Stress drop	$\Delta\tau$	1.00	MPa
Fault shearing stiffness	k_s	1.20×10^4	kN/m/m^2
Fault vertical stiffness	k_v	1.20×10^4	kN/m/m^2

The stress drop was uniformly set to 1 MPa, the condition in which the moment magnitude Mw, calculated from the fault displacement Δu of each element in the final state of the analysis by using Eqs. (4) and (5), with the fault surface as Σ, was close to the value observed in the actual earthquake. τ_y was established according to Eq. (6), referring to Andrew [8].

$$M_0 = \int_\Sigma \mu \Delta u dS \tag{4}$$

$$Mw = \frac{2}{3} \log_{10} M_0 - 6.1 \tag{5}$$

$$\tau_y = 1.6\Delta\tau \tag{6}$$

The maximum frequency which can be covered by the mesh f_{max}, that is calculated in Eq. (7), is 0.875 Hz when $n = 4$. However, β is the shear wave velocity at the crust.

$$f_{max} = \frac{\beta}{n\Delta L} \tag{7}$$

The analysis was a consecutive nonlinear response analysis according to the Newmark-β method (parameter $\beta = 0.25$, $\gamma = 0.5$). The integration time of the analysis Δt was 0.01 s, and the duration T was 20 s.

4 Analytical Results

The analytical results are shown. The simulation analysis matched well when initial stress direction λ is 60°. So deformation diagram, fault rupture time, fault displacement only the case is shown as a representative case.

4.1 Model Deformation Diagram

The deformation diagram of the analysis final time is shown in Fig. 5.
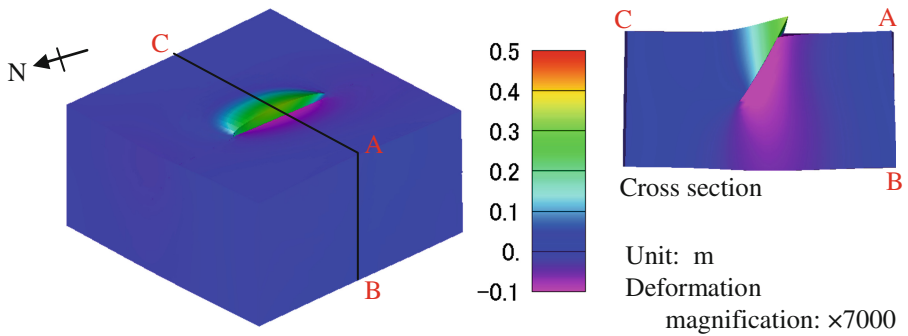

Fig. 5. Analysis model deformation diagram and vertical displacement contour diagram.

4.2 Fault Rupture Time and Fault Displacement

A contour diagram of the time that each joint element of the fault surface ruptured is shown in Fig. 6(a). The average rupture propagation time V_r was evaluated as 3 km/s from Fig. 6(a), and the S-wave speed β at the crust was 3.46 (km/s); therefore, the ratio V_r/β equals 0.87. According to recipe [9], the general ratio V_r/β is 0.72, but the fact that larger values have been obtained is also described, so the results of this test are not believed to greatly diverge from the reality. Also, the rupture propagation speed has been confirmed to increase as a result of changing the surface energy required at the time of rupture (See Fig. 3).

Contour diagrams of the fault displacement that occurred in the joint elements in the analysis final time are shown in Fig. 6(b). The seismic moment M_0, which is the index of the size of the earthquake, computed from the fault displacement of the final time was 2.77×10^{18} Nm, and the moment magnitude Mw calculated from M_0 was 6.2. This agreed well with the results for the actual earthquake according to the CMT analysis presented by the Japan Meteorological Agency in which the seismic moment was 2.98×10^{18} Nm and the moment magnitude was 6.2.

(a) Fault rupture time   (b)Fault displacement
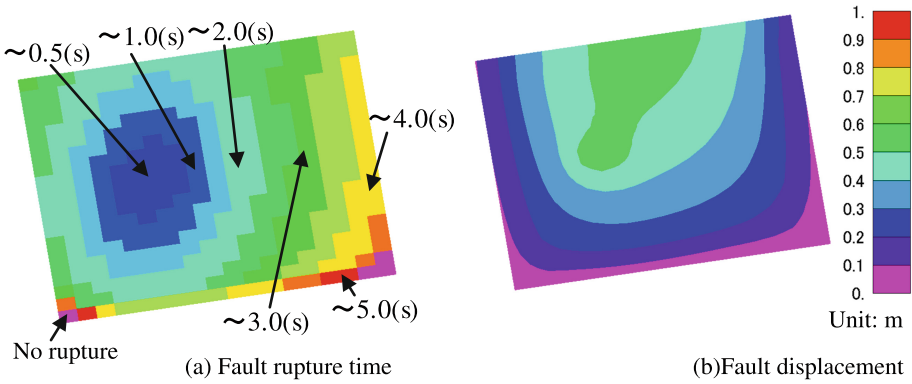
Fig. 6. Fault rupture time and fault displacement.

In addition, the surface displacement of the final time was approximately 62 cm, and the vertical displacement observed for the actual earthquake after it had occurred was approximately 90 cm. Therefore, the simulation was believed to have simulated the actual phenomenon well.

4.3 Response Time History

The response time history at the observation point location was compared with the results actually observed by K-NET Hakuba, the response acceleration on the ground surface. In this study, the displacement time history was compared to focus on the relatively long-term results. So we can neglect the effect of the surface layer. The acceleration response time history of K-NET Hakuba was corrected by using the method of Boore et al. [10], and the displacement time history waveform that were obtained by time integration were compared with the waveform obtained in the analysis. A comparison of the displacement time history obtained from the observational records with the
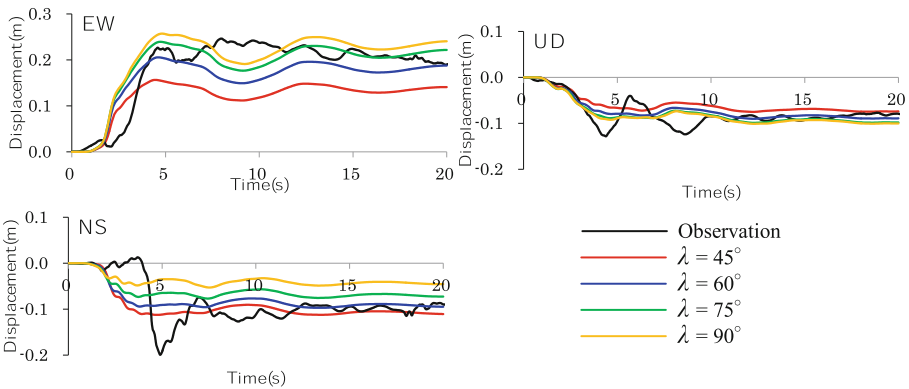
Fig. 7. Comparison of displacement response time history. (Color figure online)

analytical results is shown in Fig. 7. However, the time axis origin has been adjusted as appropriate.

Because the observation points of K-NET Hakuba were relatively close to the fault, a relatively large, permanent displacement occurred in the analysis final time. The simulation analysis matched well when initial stress direction is 60°.

5   Conclusion

A fault dynamic simulation analysis of the Kamishiro fault earthquake in Nagano Prefecture was performed using the finite element method. By adjusting the stress drop $\Delta\tau$, analytical results close to the seismic moment in the actual earthquake were able to be obtained, and the results for the surface fault displacement and displacement time history matched well with the observations of the actual earthquake. In the future, a more comprehensive study that includes a more detailed fault shape and physical property value variations is desired.

References

1. Dan, K., Muto, M., Torita, H., Ohhashi, Y., Kase, Y.: Basic examination on consecutive fault rupturing by dynamic rupture simulation. In: Annual Report on Active Fault and Paleoearthquake Researches, no.7, pp. 259–271 (2007). (In Japanese)
2. Mizumoto, G., Tsuboi, T., Miura, F.: Fundamental study on fault rupture process and earthquake motions on and near a fault by 3D-FEM. J. JSCE, no.780, I-70, 27–40 (2005). 1 (In Japanese)
3. Japan Association for Earthquake Engineering: Report about the Earthquake at the Nagano Prefecture north in 2014 (2015). (In Japanese)
4. National Research Institute for Earth Science and Disaster Prevention: Strong-motion Seismograph Networks. http://www.kyoshin.bosai.go.jp/. Accessed 01 Aug 2015
5. FrontISTR Workshop HP. http://www.multi.k.u-tokyo.ac.jp/FrontISTR/. Accessed 01 Aug 2015 (In Japanese)
6. Goodman, R.E.: Methods of geological engineering in discontinuous rocks, Chap. 8, pp. 300–368. West Publishing Company (1976)
7. National Institute of Advanced Industrial Science and Technology: Active fault data base. https://gbank.gsj.jp/activefault/index_gmap.html. Accessed 01 Aug 2015 (In Japanese)
8. Andrews, D.J.: Rupture velocity of plane strain shear cracks. J. Geophys. Res. **81**, 5679–5687 (1976)
9. Earthquake Research Committee, Headquarters for Earthquake Research Promotion, Strong motion forecasting method of the earthquake which specified an earthquake source fault (Recipe). Revision on 21 Dec. 2009 (In Japanese)
10. Boore, D.M., Stephens, C.D., Joyner, W.B.: Comments on baseline correction of digital strong-motion data: examples from the 1999 Hector Mine, California, Earthquake. Bull. Seismol. Soc. Am. **92**(4), 1543–1560 (2002)